# Mathematical and Experimental Modelling of Sorption Processes in a Fixed Bed Adsorber*

M. ŠOÓŠ**, P. RAJNIAK, and R. ŽAJDLÍK

*Department of Chemical and Biochemical Engineering, Faculty of Chemical Technology,*
*Slovak University of Technology, SK-812 37 Bratislava*
*e-mail: soos@cvt.stuba.sk*

The aim of this work was to present experimental sorption measurements and elution curves for the system silica gel—water vapour, which is characteristic by capillary condensation. The experiments were performed at different temperatures, flow-rates of inert gas, and different relative humidities. It was found that with increasing temperature the plateau in the plot of relative humidity *vs.* time moved to lower values of relative humidity and the time of the experiment decreased. The phenomenon of capillary condensation – hysteresis in adsorption-desorption isotherms was manifested for the temperature up to 94 °C and very likely it exists at temperatures higher than the boiling point. A comparison of experimental measurements and the solution of a mathematical model further was presented for the fixed bed with axial dispersion. The results from the solution of this model neglecting capillary condensation were very different from the experimental measurements. This also confirmed the need to consider the phenomenon of capillary condensation.

A fixed bed adsorber is the mostly used system in sorption processes. This configuration is very simple from the construction viewpoint but the mathematical model is complicated. The aim of this work is to present experimental sorption measurements and elution curves obtained in a fixed bed adsorber. The phenomenon of capillary condensation is manifested not only in the curvature of the adsorption-desorption isotherm but also in the shape of the elution curve in the course of the process. Systems with vapour adsorbates can exhibit capillary condensation caused by the interaction of porous solid with the condensable vapour. Capillary condensation is usually manifested when the ratio of the partial pressure above the meniscus to the partial pressure above the straight surface is equal to 0.4 [3]. A consequence is that for the desorption equilibrium the adsorbed amount is higher than for the adsorption equilibrium (Fig. 1). The phenomenon of capillary condensation can be explained using two models, the independent pore model and the pore-blocking model. The pore-blocking theory [4, 7, 8] was developed directly for the capillary condensation domain and it describes the adsorption-desorption equilibria for the relative pressure between $x^L$ lower limiting point and $x^U$ upper limiting point, as shown in Fig. 1.
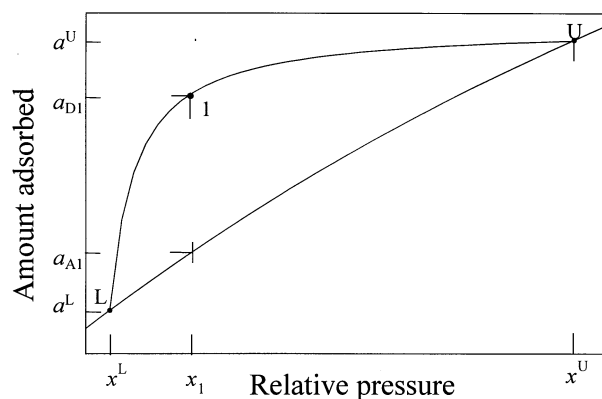


**Fig. 1.** Adsorption-desorption isotherm for the system silica gel—water vapour. The comparison of the theoretical (infinite system) and the experimental (finite system) amount adsorbed.

A comparison between the solutions of a mathematical model of a fixed bed with or without hysteresis is presented in this work. The results from the solutions neglecting capillary condensation are very different from the experimental measurements. This means that the above-mentioned phenomenon must be taken into account.

---

*Presented at the 27th International Conference of the Slovak Society of Chemical Engineering, Tatranské Matliare, 22—26 May 2000.
**The author to whom the correspondence should be addressed.

## THEORETICAL

### Models of Mass Transport in the Single Microparticle

This model pictures the particle as consisting of a solid phase interspersed with pores, but with the adsorbate diffusing in the pore voids only, and the adsorption occurring at the internal surface. The adsorbed molecules are immobilized and can migrate only by desorbing first.

The mathematical model of adsorption or desorption in a single particle of sorbent assumes that the main mechanism of material transport in a single particle is diffusion in the liquid phase in pores of a sorbent (pore diffusion) and pore diffusion model consists of the following relations:

Mass balance for the spherical particle

$$\frac{\partial a}{\partial t} + P\frac{\partial c}{\partial t} = D_P\left(\frac{\partial^2 c}{\partial r^2} + \frac{2}{r}\frac{\partial c}{\partial r}\right) \qquad (1)$$

Boundary conditions for the particle

$$t \geqq 0 \quad r = 0 \quad \frac{\partial c}{\partial r} = 0 \qquad (2)$$

$$r = R \quad D_P\frac{\partial c}{\partial r} = k_g(C - c^S) \qquad (3)$$

Initial conditions for the particle

$$t < 0 \quad 0 \leqq r \leqq R \quad c = c_i \qquad (4)$$

Equilibrium isotherms for adsorption

$$a_A = a_{mA}\frac{K_A c}{1 + K_A c} \qquad (5)$$

and for desorption

$$a_D = a^L + a_{mD}\frac{K_D(c - c^L)}{1 + K_D(c - c^L)} \qquad (6)$$

The isotherm equations and parameters for equilibrium isotherms are taken from [7] and all parameters of the mathematical model are listed in Table 1.

### Mathematical Model of Adsorption and Desorption in a Fixed Bed

There are various different mathematical models for adsorption and desorption processes in a fixed bed. *Yang* [11] presented in his book some examples of models for fixed bed adsorption processes at isothermal conditions. The simplest models without axial and radial dispersion, with constant diffusivity and linear isotherm, and their exact solutions have been discussed. *Hwang et al.* [1] used the same models for a fixed bed without axial and radial dispersion, but with

nonisothermal conditions. *Sun* and *Meunier* [9] presented the finite difference method for fixed bed multicomponent sorption. The authors solved the sorption process by a mathematical model for fixed bed with axial dispersion at nonisothermal conditions. *Chatzopoulos* and *Varma* [2] introduced the solution of aqueous-phase sorption of toluene in fixed beds of activated carbon. They used the isothermal model with the absence of axial and radial dispersion, and the surface diffusion model for a sorbent particle with the surface diffusivity increasing exponentially with surface concentration. The model solution was in a good agreement with the experiment.

In our work, we used the mathematical model with axial dispersion in the fixed bed, isothermal conditions and the pore diffusion model for a sorbent particle.

Mass balance for the adsorptive in the bed voids

$$\varepsilon\left[\frac{\partial C}{\partial t} + w\frac{\partial C}{\partial z}\right] + a_P k_g(C - c^S) = D_L\frac{\partial^2 C}{\partial z^2} \qquad (7)$$

Boundary conditions for the fixed bed in axial direction

$$t = 0 \quad z = 0 \quad \varepsilon w(C - C^{in}) = D_L\frac{\partial C}{\partial z} \qquad (8)$$

$$z = L \quad \frac{\partial C}{\partial z} = 0 \qquad (9)$$

Initial conditions for the fixed bed are generally in the following form

$$t \leqq 0 \quad 0 \leqq z \leqq L \quad C = C_i \qquad (10)$$

The material balance for the fixed bed must be combined with the material balance for a single adsorbent particle (eqns (1—4)). For adsorption-desorption equilibria with hysteresis the parameters in eqns (5, 6) are different for adsorption and desorption [7, 8]. Parameters of mathematical model are listed in Table 1.

### Numerical Solution

Both the sets of equations for the single particle and the gas phase in the column can be recognized to be belonging to the case of second-order parabolic differential equations of the boundary value type coupled with one another. The technique used in this paper makes use of the "orthogonal collocation method" to reduce them all into a set of first-order ordinary differential equations.

The single particle problem is solved first. The partial differential equation (eqn (1)) and boundary conditions (eqns (2, 3)) are rewritten at $N$ selected radial positions in the particle according to the orthogonal collocation method [5, 10]. In this way the single particle equations are reduced to $N$ coupled ordinary differential equations containing $N + 2$ unknowns. The extra one unknown is the concentration of the fluid

**Table 1.** Parameters of the Adsorber and Properties of the System Silica Gel—Water Vapour

| | | | |
|---|---|---|---|
| $L/\text{m}$ | 0.29 | $a_{\text{mA}}/(\text{mol m}^{-3})$ | $5.386 \times 10^4$ |
| $a_{\text{P}}/(\text{m}^2 \text{ m}^{-3})$ | 1188.3 | $K_{\text{D}}/(\text{m}^3 \text{ mol}^{-1})$ | 38.709 |
| $\varepsilon$ | 0.287 | $a_{\text{mD}}/(\text{mol m}^{-3})$ | $9.853 \times 10^3$ |
| $w/(\text{m s}^{-1})$ | 0.207 | $a^{\text{L}}/(\text{mol m}^{-3})$ | $1.191 \times 10^4$ |
| $P$ | 0.42 | $c^{\text{L}}/(\text{mol m}^{-3})$ | 0.362 |
| $d_{\text{P}}/\text{m}$ | $3.6 \times 10^{-3}$ | $D_{\text{g}}/(\text{m}^2 \text{ s}^{-1})$ | $21.4 \times 10^{-6}$ |
| $\rho_{\text{P}}/(\text{kg m}^{-3})$ | 1249.0 | $D_{\text{P}}/(\text{m}^2 \text{ s}^{-1})$ | $2.29 \times 10^{-6}$ |
| $\rho_{\text{g}}/(\text{kg m}^{-3})$ | 1.185 | $D_{\text{L}}/(\text{m}^2 \text{ s}^{-1})$ | $7.81 \times 10^{-3}$ |
| $K_{\text{A}}/(\text{m}^3 \text{ mol}^{-1})$ | 0.783 | $k_{\text{g}}/(\text{m s}^{-1})$ | 0.0795 |

Experimental conditions: flow-rate 120 dm$^3$ h$^{-1}$, $\theta = 24\,°\text{C}$.

surrounding the particle. For the single particle problem we introduce $c^{\text{S}} = C$ and then $N$ equations with $N$ unknowns can be integrated.

For the fixed bed problem concentration is obtained from the external field equation. The orthogonal collocation method is also used to reduce eqn (7) with the boundary condition (eqns (8, 9)) to an ordinary differential equation. The partial differential equation is rewritten at $M$ selected axial positions in the adsorber. In this way both partial differential equations are split into $M + MN$ first-order ordinary differential equations containing the same number of unknowns. All equations are solved simultaneously using the semiimplicit third-order "Runge—Kutta method" [5, 10]. Because the coefficient matrix of the equation set for the fixed bed problem has very sparse structure the modified LU decomposition routine for sparse systems may be used. In this work we employed an optimal "Crout algorithm" for sparse systems of linear algebraic equations with constant structure matrix. Thus a drastic reduction in computer time was achieved. The number of collocation points used was varied until the accuracy of the obtained profiles remained essentially unchanged. For computations, seven collocation points in the external field and four in the pellet radius including boundary points have been used to give a satisfactory accuracy that is until the third significant digit, *i.e.* $M = 5$ and $N = 3$ and $5 + 5 \times 3 = 20$ equations were simultaneously integrated. The whole simulation could be performed in about 1 min on a Pentium II, 400 MHz computer.

*Model of Equilibrium Adsorption or Desorption*

Supposing that the adsorption (desorption) equilibrium in the fixed bed is immediately reached, we can speak about equilibrium adsorption (desorption). The elution time for equilibrium adsorption is equal to the stoichiometric time, which can be calculated as follows

$$t_{\text{st}} = \frac{L(1 - \varepsilon)(a_0 - a_1)}{\varepsilon w(c_0 - c_1)} \qquad (11)$$

This stoichiometric time can be used as a control of the material balance not only for the experiment but also for the mathematical model.

## EXPERIMENTAL

Silica gel, Davidson Grade H standard commercial desiccant, was used. Both the specific BET surface area and the pore volume for silica gel were determined by SORPTOMATIC 1900 (Fisons, Rodano, Milan, Italy) apparatus to be 767 m$^2$ g$^{-1}$ and 0.398 cm$^3$ g$^{-1}$, respectively. For the measurement in the fixed bed, the apparatus depicted in Fig. 2 was used. This apparatus consists of three parts: preparation of the inlet air, adjustment of the mixture air/water, and fixed bed adsorber.

The adsorber was divided into three parts. The lower and upper parts were filled with glass spheres, the middle part was filled with silica gel. A glass tube was placed in the axis of the adsorber. Inside of this tube, two thermocouples were placed. The tempered adsorber was used. A combined probe HTS 57 (ČKD POLOVODIČE a.s., Prague, Czech Republic) was used for the measurement of the relative humidity and the temperature of air. The probe was designed for continuous measurements of the relative humidity and temperature of gaseous nonaggressive media. The principle of measurement was based on the change of the probe dielectric permittivity by water molecules. All measured data were monitored on the display and at the same time recorded in the computer.

A thermocouple (type Fe/Co) was employed for the measurement of temperature in the fixed bed. The temperature was recorded in the computer. The relative error of the temperature measurement was 0.75 %.

The rotameter (ROTA YOKOGAWA, Wehr, Germany) was used for the measurement of the gas flow-rate. The flow-rate of pure air was assumed to be the same as the flow-rate of the mixture air—water vapour. The rotameter was recommended for the measurement of air at a temperature of 20 °C and pressure 101.325 kPa. The relative error of the gas flow measurement was 2 %.

Water for the system was dosed by a peristaltic pump (ISMATEC, Zurich, Switzerland). The plastic tube was deformed during the experiment and therefore, we had to measure the flow-rate before and after each experiment. The average flow-rate was used in mathematical modelling.
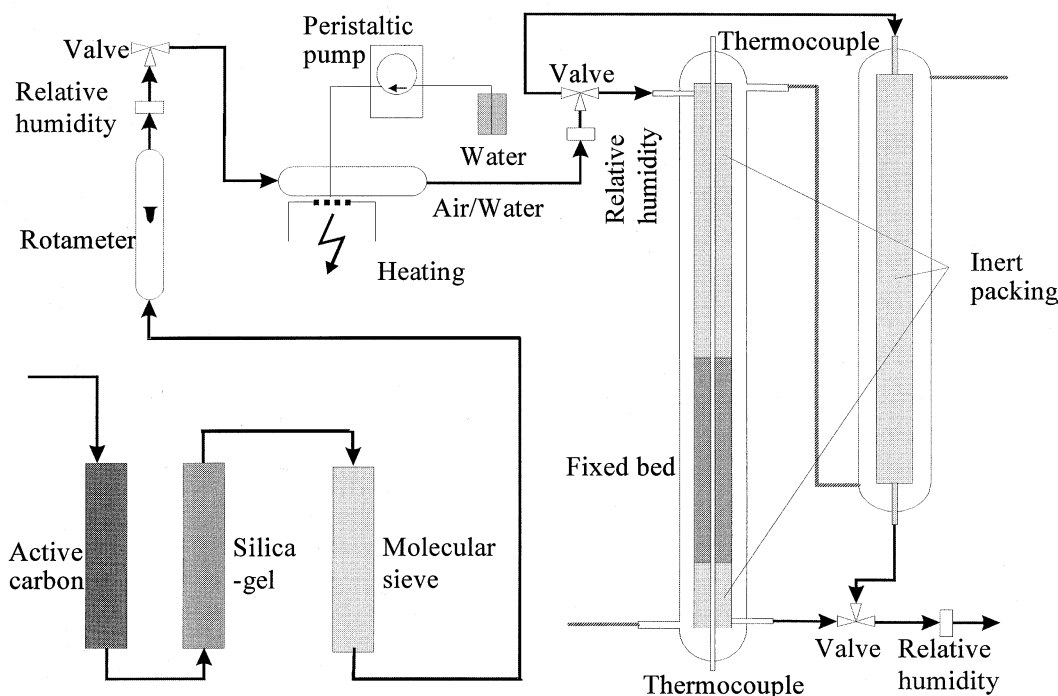
Each experiment consisted of adsorption and des-

**Fig. 2.** Experimental apparatus for the measurement in the fixed bed.

orption cycles. We adjusted the flow-rates of air and water and this mixture was first put through a bypass. When the relative humidity reached a steady state, the flow through the adsorber was changed and the experiment started. When the adsorption was finished, the flow was switched to a bypass and the flow-rate of water was measured. Then, the value of the relative humidity for desorption was adjusted. The flow of air was changed and desorption could start.

The experimental conditions were: the flow-rate of air within the range of 120—360 dm$^3$ h$^{-1}$, temperature 16—94 °C, and relative humidity of air within the range of 0—100 %.

## RESULTS AND DISCUSSION

Experimental measurements of adsorption and desorption were performed for different values of temperature, air flow-rate, and relative humidity. A comparison of experimental adsorption measurements and the solution of the mathematical model, given by eqns (1—10) is shown in Fig. 3. The experimental flow-rate was 120 dm$^3$ h$^{-1}$ and the temperature 24 °C. The predicted stoichiometric time was in a good agreement with the experiment. Some differences between the solution of the mathematical model for the fixed bed and the experiment could be caused by the assumptions of constant diffusivity, isothermal conditions, and constant voidage of the bed.

Fig. 4 shows the time dependence of temperature for adsorption at the inlet and at the outlet of the fixed bed where a rapid increase of temperature at the front
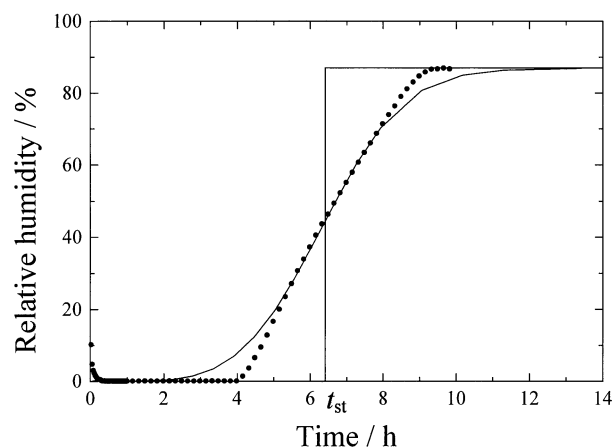


**Fig. 3.** Comparison of concentrations at the output of the fixed bed obtained from experimental measurements (●) and from the mathematical model (—) at $\theta$ = 24 °C and flow-rate 120 dm$^3$ h$^{-1}$.

of the fixed bed and a slow increase at the end of the fixed bed are shown. This fact is in conflict with the assumption considered in the mathematical model.

Fig. 5 illustrates the experimental adsorption in the fixed bed and the stoichiometric time computed from using eqn (11). The shape of the sorption curve in this figure was rather different from that one in Fig. 3. This is caused by impact of different flow-rate on both, the axial dispersion coefficient and the mass transfer coefficient.

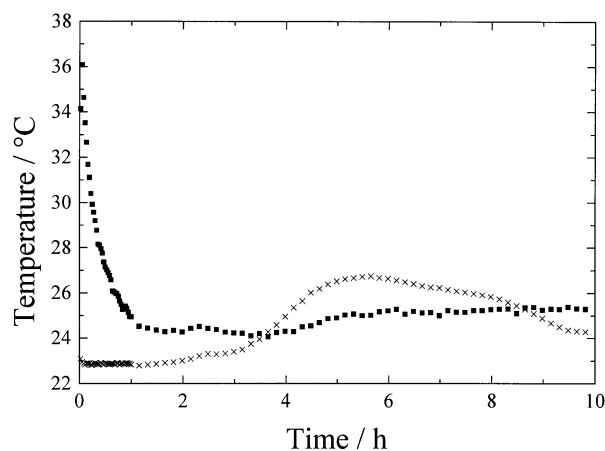Fig. 6 presents the experimental elution curves and the solution of the mathematical model for systems

**Fig. 4.** Time dependence of temperature in the fixed bed during adsorption, inlet of the fixed bed (■), outlet of the fixed bed (×); experimental conditions: $\theta = 24\,°C$, flow-rate 120 $dm^3$ $h^{-1}$.
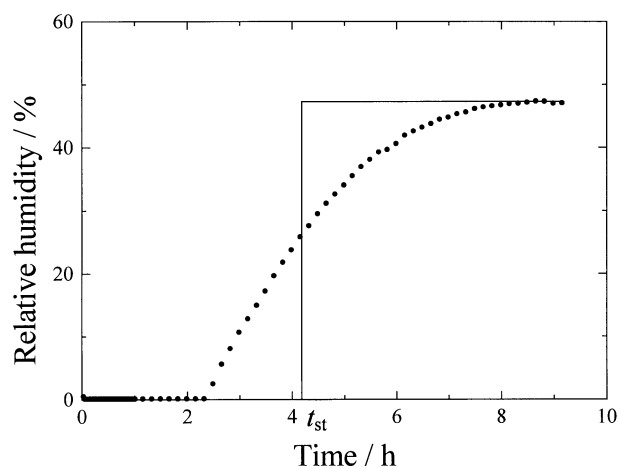


**Fig. 5.** Sorption curve at the air flow-rate 240 $dm^3$ $h^{-1}$ and the temperature $\theta = 24\,°C$ (●).



**Fig. 6.** Comparison of elution curves obtained by experimental measurements (■) and by the mathematical model with the adsorption-desorption hysteresis loop, eqn (6) (—) or by the mathematical model with the adsorption-desorption isotherm without hysteresis, eqn (5) (− − −); experimental conditions: $\theta = 24\,°C$, flow-rate 120 $dm^3$ $h^{-1}$.



**Fig. 7.** Time dependence of temperature in the fixed bed during desorption, inlet of the fixed bed (—), outlet of the fixed bed (●); experimental conditions: $\theta = 24\,°C$, flow-rate 120 $dm^3$ $h^{-1}$.

with or without hysteresis. As one can see, the solution with hysteresis predicted well the value of relative humidity at the plateau of the elution curve as well as the time scale of the plateau. The solution for the system without hysteresis can provide wrong results for the desorption. The differences between the experiment and the solution of adsorption-desorption model with hysteresis were probably caused by assuming constant diffusivity in the whole range of relative humidity and isothermal conditions in the model [6]. Fig. 7 shows the time dependence of temperature for desorption at the inlet and at the outlet of the fixed bed where a rapid decrease of temperature at the front of the fixed bed and a slow decrease at the end of the fixed bed are shown.

Elution curves for different flow-rates and temperatures are illustrated in Figs. 8—11. In all experiments, a plateau with approximately equal value of
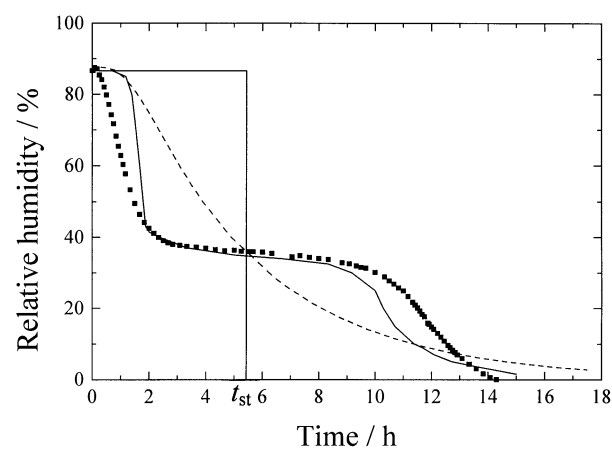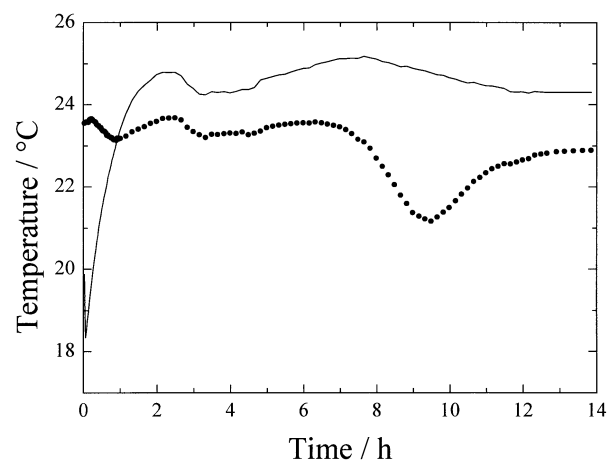
relative humidity occurred. The temporal length of this plateau was a function of flow-rate and temperature. The length of this plateau decreased with increasing flow-rate. The same effect was observed at temperature. These experiments confirmed that the adsorption-desorption hysteresis for the system silica gel—water vapour exists in the whole range of temperatures, 16—94 °C, and at all values of flow-rate used in this study. Theoretically, the phenomenon of capillary condensation and hysteresis can exist also at a temperature higher than the boiling point. With increasing temperature, the relative humidity corresponding to the plateau moves towards lower values. This also means a decrease of the value of the lower limiting
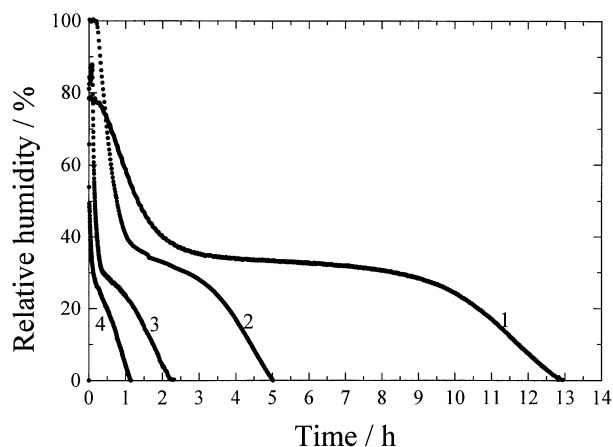
**Fig. 8.** Comparison of elution curves for the flow-rate of air 120 dm³ h⁻¹ at different temperatures $\theta$: 24 °C (*1*), 40 °C (*2*), 60 °C (*3*), 70 °C (*4*).
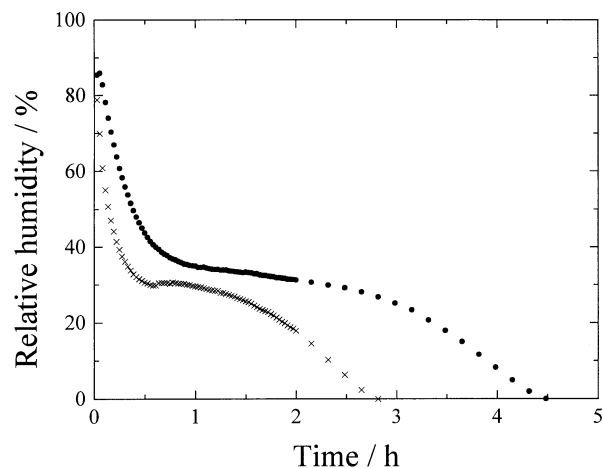


**Fig. 10.** Comparison of elution curves for the flow-rate of air 40 dm³ h⁻¹ at different temperatures $\theta$: 60 °C (●), 70 °C (×).
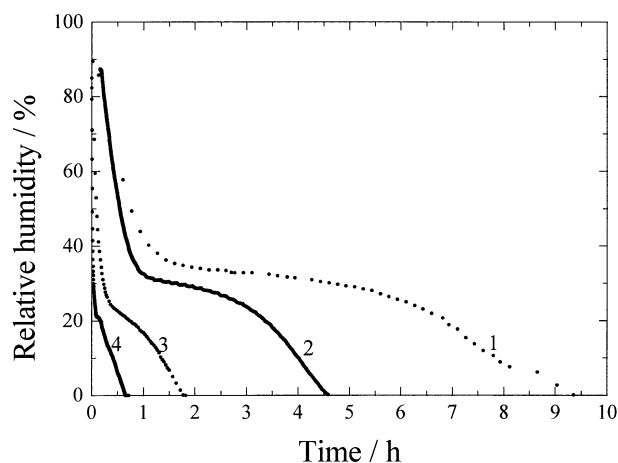


**Fig. 9.** Comparison of elution curves for the flow-rate of air 360 dm³ h⁻¹ at different temperatures $\theta$: 16 °C (*1*), 24 °C (*2*), 40 °C (*3*), 60 °C (*4*).
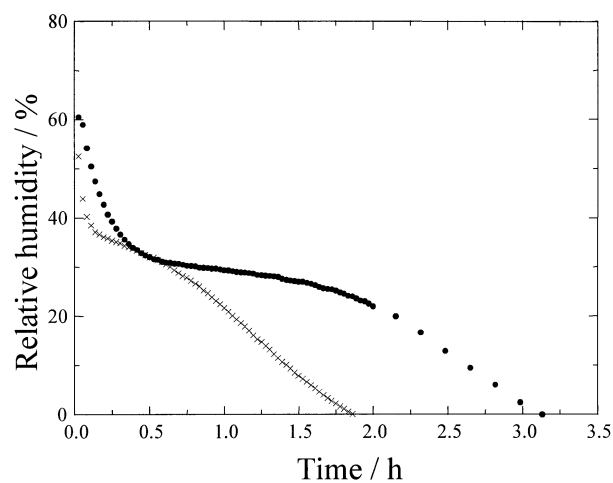


**Fig. 11.** Comparison of elution curves for the flow-rate of air 20 dm³ h⁻¹ at different temperatures $\theta$: 80 °C (●), 94 °C (×).

point for the primary desorption curve in Fig. 1. This effect was not confirmed at the highest experimental temperatures of 80 °C and 94 °C (Fig. 11). This could be caused by a low air flow-rate. This discrepancy had, however, no effect on that the capillary condensation-hysteresis phenomenon existed at this temperature. The existence of hysteresis and its shape at different temperatures should be confirmed by equilibrium measurements.

## CONCLUSION

In this work experimental sorption measurements and elution curves for a fixed bed adsorber were presented. As a test system silica gel—air—water vapour was chosen. This system is characteristic by adsorption-desorption isotherms with hysteresis. The effects of different flow-rates of inert gas, tempera-

tures, and relative humidities on the desorption curves were investigated. We can say that the increasing flow-rate decreases the time of desorption for the same starting conditions. The increase of temperature has the same effect and the relative humidity corresponding to the plateau moves towards lower values. These results indicated that the capillary condensation phenomenon existed at all temperatures including those close to the boiling point of water.

The solution of a mathematical model was in a good agreement with experimental measurements when the hysteresis in the sorption isotherm was incorporated in the model. If the hysteresis was neglected, great differences between the model solution and the experiment appeared. The concentration dependence of the diffusivity should be considered for a better agreement of the mathematical model and experiments.

## SYMBOLS

| | | |
|---|---|---|
| $a$ | concentration of adsorbate in the adsorbed phase | mol m$^{-3}$ |
| $a_m$ | parameter of the isotherm | mol m$^{-3}$ |
| $a_P$ | $6^*(1-\varepsilon)/d_P$, specific area of particle surface | m$^2$ m$^{-3}$ |
| $C$ | concentration of adsorbate in the fluid phase | mol m$^{-3}$ |
| $c$ | concentration of adsorbate in the pores of adsorbent | mol m$^{-3}$ |
| $d_P$ | particle diameter | m |
| $D_L$ | axial dispersion coefficient in the bed | m$^2$ s$^{-1}$ |
| $D_P$ | effective diffusivity of the pore diffusion | m$^2$ s$^{-1}$ |
| $k_g$ | mass-transfer coefficient | m s$^{-1}$ |
| $K$ | parameter of the isotherm | m$^3$ mol$^{-1}$ |
| $L$ | adsorber length | m |
| L | lower limiting point in the adsorption-desorption isotherm (Fig. 1) | |
| $M$ | number of internal collocation points in the bed | |
| $N$ | number of internal collocation points in the particle | |
| $P$ | particle porosity | |
| $R$ | particle radius | m |
| $r$ | space coordinate in the particle | m |
| $t$ | time | s |
| $\theta$ | temperature, Figs. 3—11 | °C |
| U | upper limiting point in the adsorption-desorption isotherm (Fig. 1) | |
| $w$ | intraparticle space velocity | m s$^{-1}$ |
| $z$ | axial coordinate in the fixed bed | m |
| $x$ | relative pressure | |

## Subscripts

| | |
|---|---|
| A | adsorption |
| D | desorption |
| i | initial condition |
| st | stoichiometric |
| g | fluid phase |
| 0 | starting condition, eqn (*11*) |
| 1 | finishing condition, eqn. (*11*) |
| 1 | point in Fig. 1 |

## Superscripts

| | |
|---|---|
| in | inlet condition |
| L | lower limiting point, Fig. 1 |
| S | surface condition |
| U | upper limiting point, Fig. 1 |

## Greek Letters

| | |
|---|---|
| $\varepsilon$ | voidage of the bed |

## REFERENCES

1. Hwang, K. S., Jun, J. H., and Lee, W. K., *Chem. Eng. Sci. 50*, 813 (1995).
2. Chatzopoulos, D. and Varma, A., *Chem. Eng. Sci.*, *50*, 127 (1995).
3. Kellö, V. and Tkáč, A., *Physical Chemistry* (in Slovak). Alfa Publishers, Bratislava, 1982.
4. Mason, G., *Proc. R. Soc. London 41*, 453 (1988).
5. Rajniak, P. and Ilavský, J., *Adsorption Sci. Technol. 3*, 232 (1986).
6. Rajniak, P., Šoóš, M., and Yang, R. T., *AIChE J. 45*, 735 (1999).
7. Rajniak, P. and Yang, R. T., *AIChE J. 39*, 774 (1993).
8. Rajniak, P. and Yang, R. T., *AIChE J. 40*, 913 (1994).
9. Sun, L. M. and Meunier, F., *AIChE J. 37*, 244 (1991).
10. Villadsen, J. and Michelsen, M. L., *Solution of Differential Equation Models by Polynomial Approximation.* Prentice Hall, Englewood Cliffs, NJ, 1978.
11. Yang, R. T., *Gas Separation by Adsorption Processes.* Butterworth, Boston, 1987.